The tests were carried out on 5000kN reaction frame in the Construction Engineering Laboratory of Shenyang Jianzhu University. Because the intent was to examine the force transfer mechanism in the ring stiffener in detail, the specimens were extensively instrumented with strain gages, as shown in Figs. 2 and 3. Rosette strain gauges were glued to the surface of the ring stiffeners at locations 45º and 90º degrees from the beam axis with the R and H gages aligned radially and tangentially to a line from the center of the column. Similar rosettes were used in the tube and beam web (Fig. 4). Longitudinal gages were used in the beam flanges.

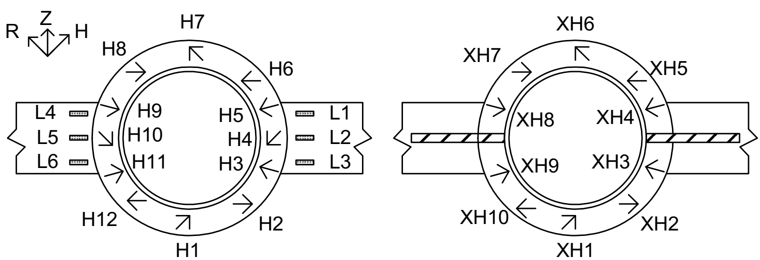

Fig.2 Position of the strain gauges in the beams and ring stiffeners

To start the tests, a 1800kN axial compressive force was applied to the top of the concrete-filled steel tube using a 5000kN jack. This axial load corresponded to about 0.6 of the nominal axial strength of the column and was maintained through the whole experiment[11-13]. Vertical reversed low cyclic loads were then imposed on the steel beams by electro-hydraulic actuators.

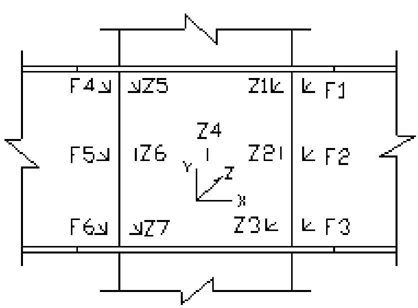

Fig.3 Position of the strain gauge in the joint

For the exterior joint, the initial load was 10kN with 5kN added at each new load level. The specimen was cycled 3 times at each of these load levels until the load reached

160kN; afterwards, the test was controlled by beam end displacements, in increments of 2mm, until the load reached 280kN when the joint failed. For the interior joint, displacement control was used for the whole experiment. The initial displacement was 3mm, and 2mm were added at every displacement increment, which consisted of 3 cycles. After yield was reached, the displacement change was increased to 3mm and only 2 cycles were applied until the load reached 250kN when the joints failed.

The load vs. beam end displacement curves are shown in Fig.4. Each 10mm of beam end displacement corresponds to about 1.25% interstory drift. It can be seen from Fig.4 that the curves are full, indicating the joints have excellent energy dissipation and hysteretic behavior. The large number of cycles imposed is also obvious from the figures.

After the joints yield (200kN), the two cycles at each deformation level almost coincide and the strength and stiffness decline very gradually. Overall, the joints are characterized by excellent ductility. The right beam for the interior joint showed a somewhat higher strength (250 kN) in the positive, or initial, direction of loading. In general, every 3mm increment resulted in a load increase of about 6.5kN until failure occurred due to fractures of the welds at the beam-ring interface. It should be noted that given the large number of cycles imposed, the total energy dissipated and the summation of the local plastic strains at the welds was large. An assessment of the significance of the weld failure at a relatively low interstory drift (2.5%) needs to take this into account.

3 Analysis of strain data

Fig. 5 shows the strain profiles across the flanges of the one interior and the exterior beam at three positions (refer Fig. 2 for gage locations). Before the load reached ±100kN, the strain values at the three locations are basically the same in the first direction of loading (positive load). When the load is between ±100kN and ±160kN, strain values at the three locations change differently, particularly in the negative direction of loading, but all maintain a straight line trend. When the load reaches ±160kN, the specimen starts to yield, and the strains increase rapidly as the steel beam enters the elastic-plastic stage. With additional loads beyond ±160kN, the plastification of the specimen is becoming obvious. The strain increment also increases along with until the load reaches ±220kN when the local strain value begins to stabilize, yielding extends, and a full plastic hinge forms.

Throughout the test, the longitudinal strains in the steel beam flanges increase gradually and predictably. The strain data indicates a reasonably uniform distribution of strains across the flange and the formation of a full plastic hinge in the positive direction of loading (downwards) but a pronounced asymmetry and lack of yielding in the negative direction. This appears to be due to incipient lateral torsional buckling.

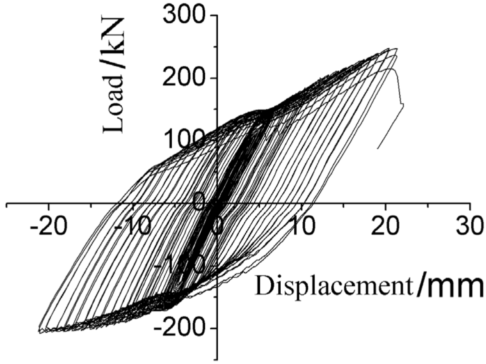

(a) Right beam (interior joint)

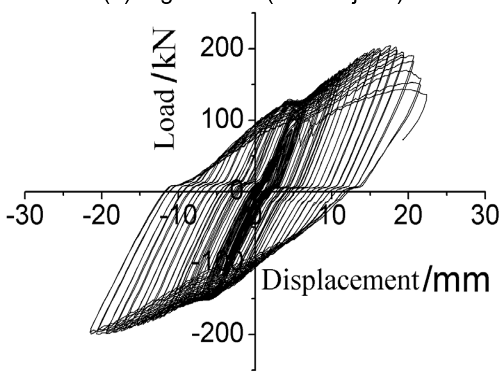

(b) Left beam (interior joint)

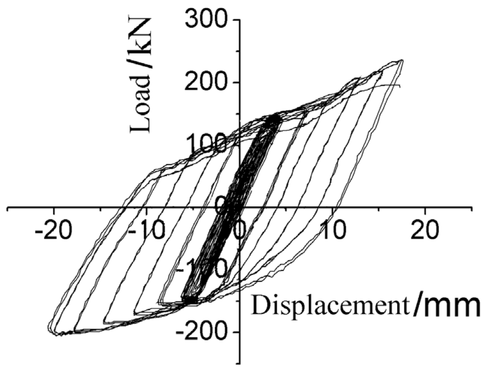

(c) Exterior joint

Fig.4 Load-beam end displacement curve

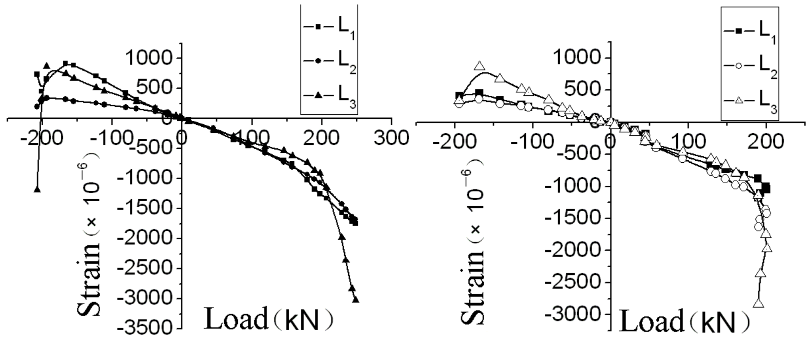

(a) Interior joint - Right beam (b) Exterior joint

Fig.5 Strains in the flanges of the steel beams

Fig.6 shows the strains in the web of the beam (refer to Fig.3 for strain gauge locations). The shape of the strain distribution for the interior and exterior joints is similar. The magnitude of the maximum strains is also close, and these strains are consistent with those in the steel beam flanges. The change of the strain value at F1-X and F3-X are reasonable and intuitive, while that of F2-X is not.

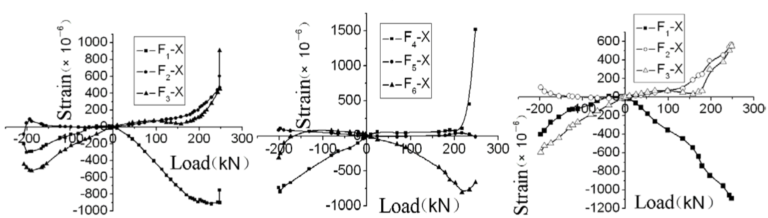

(a) Interior joint - right (b) Interior joint - left (c) Exterior joint

Fig.6 Strains in beam webs

The difference is due to the ring stiffener located close to F1-X and F3-X. The ring stiffener affects the stress distribution of the section and the stress is concentrated in this area. F2-X is far from the ring stiffener. Fig.8 shows the shapes of the strain distribution at the junction of the steel tube and the steel beam. These differ because the weld affects the strain distribution in the steel tube in this area and the geometric centerline and the loading axis of the specimen do not coincide exactly. Therefore, the axial force affects these two measuring points differently and the maximum strain values are also different. Compared with points Z1-Y, Z4-Y, Z5-Y, Z7-Y, points Z2 and Z6 changed little as the load increased. The reason is that the four measure points are close to the ring stiffener and the steel webs, where the welds are concentrated and the joint is weak. When the load reached 160kN, this is the location where the joint begins to yield.

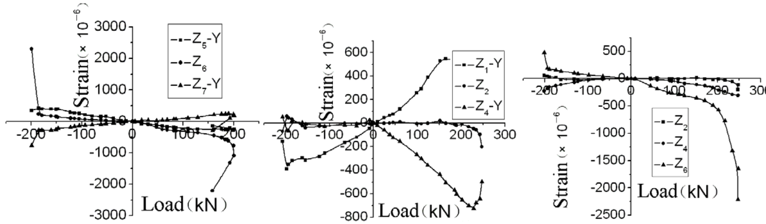

(a) Right connection (S1) (b) Left connection (S1) (c) Centreline

Fig.8 Strains in the steel tube

Point Z4 is in the center of the steel tube, and as it can be seen from Fig.8 (c), the strain changed little and showed no yield phrase. The curve just decreased(?) a little when the load reached to 250kN. This implies that that the loads on the beams have only a small affect on the strain of the center of the steel tube; the main influence is from the axially compressive force. The concrete in the steel tube is also good for the stability of the steel tube. The steel ring stiffeners symmetry was fully considered when the positions of the measurement points were selected. As can be seen from Figs. 9 and 10, the strain of the steel ring stiffeners followed the expected patterns. In Fig.9, for the top ring, gages H9-z, H10-z, H11-z, H3-h, H4-h and H5-h are above the area of the junction of the steel ring stiffener and steel beam flanges. In Fig.10, for the bottom ring, gages XH8-z, XH9-z, XH3-h and XH4-h are below the area of the junction of the steel ring stiffener and steel beam flanges.

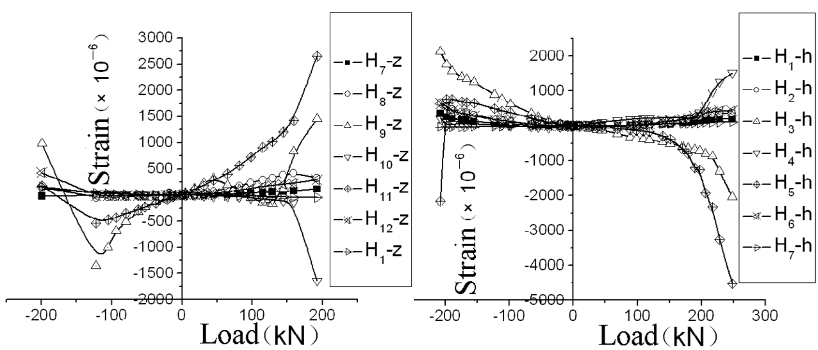

(a) Left steel ring stiffener (b) Right steel ring stiffener

Fig.9 Strain in the top steel ring stiffener

The strains of all these points changed predictably as the load increases. Points H9-z, H11-z, H3-h, H5-h, XH8-z, XH9-z, XH3-h and XH4-h, which are in near the corner of the steel ring stiffener and steel beam flanges, change rapidly after the yield value is reached. The stress in these areas is concentrated (maximum strain is 4.9×10^{-3}) and is also the position which was damaged first. Points H8-z, H12-z, H2-h, H6-h, XH7-z, H10-z, XH2-h and XH5-h are in the areas of 45° angle of the ring-flat and beam axis. The strain of these measure points also change fast but at a lower rate than the ones in the corner areas. This shows that the areas near 45° are also high stress areas. Points H1-z, H7-z, XH1-z and XH6-z are in the areas of 90° angle of the ring-flat and beam axis and their strain changes little with the load increments. The curves are linear and have no obvious influence from the beam forces. The reason is that these points are far from the center of the joints and are affected only marginally by the shear force coming from the beams.

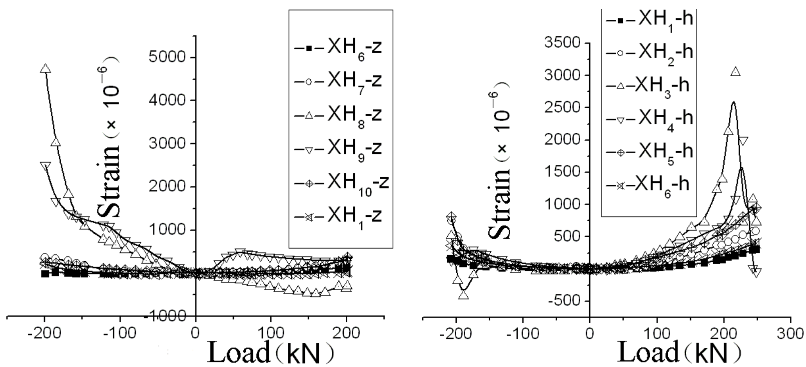

(a) Left steel ring stiffener (b) Left steel ring stiffener

Fig.10 Strain of the steel ring stiffeners below

4 Conclusions

The examination of the data obtained indicates that:

The force distribution at the center of the joints is complex and not in accord with those of a simple mechanical joint model. The behavior of other parts of the joints coincided with those from the mechanical models.

The areas up to a 45° angle of the ring are high stress areas but less so than the areas around a 0° angle to the beam. It appears that little can be done to reduce the stress concentrations in this region of the connection.

Extrapolation for the measured strains to the location of welds indicates that the strain state in these areas is complex, that high stress concentrations are likely, and that damage to the welds is likely under reversed cyclic loads.

The concrete in the steel tube is good for the stability of the steel tube. The loads on the beams affect the strain of the centre steel tube only marginally; the main effect is the axially compressive force.

Acknowledgements

The article was written while the senior author spent a sabbatical year at Georgia Tech. The support of the PRC government is gratefully acknowledged.

References

[1] ST Zhong. *Concrete-filled steel tube*. Harbin: Heilongjiang Science and Technology Press, 1995.
[2] DX Zhang, SM Zhang. Dynamic behavior of joints between concrete-filled steel tubes and beams. Journal of Harbin Jianzhu Univ., 2001,34(1):21-27.
[3] LH Han. C*oncrete-filled steel tube*. Beijing: Science Press, 2000.
[4] Beutel J., Thambirtnam D., and Perera N. Cyclic behaviour of concrete filled steel tubular column to steel beam connection. Eng. Structures, 2002, 24(11): 29-38.
[5] Li, G.C. and Liu, Z.Y. Self-Stress light-weight Concrete-filled steel tube. Shenyang: Northeastern Univ. Press, 2001.
[6] Li, G.C and Yang, H. Experimental research on the composite material mechanical properties of Self-Stress Light-weight Concrete-filled steel tube. Journal of Nanjing construction engineering college, 2001,(3): 21-25.
[7] Hao, G.Q. Research on the application of the light-weight concrete-filled steel tube. Journal of Building Materials and Application, 1999,(5): 27-32.
[8] Liu, Y.W. *Steel and concrete composite structure by manual calculation*. Beijing: China Construction Industry Press, 2004.
[9] Ge, H.B., Susantha, K.A.S., Satake Y., and Usami, T. Seismic demand predictions for concrete-filled steel box columns. Engineering Structures, 2003, 25:337~345.
[10] Zhong, S.T. *Concrete-filled steel tube in high-rise buildings*. Harbin: Heilongjiang Science and Technology Press, 1999.
[11] Huang, T. Basic research and design method for joints of concrete-filled steel tubes. Guangzhou: CE Department Huanan Polytechnic University, 2000.
[12] Mazzolani, F. *Moment resistant connections of steel frames in seismic areas -Design and reliability,* London: E & FN Spon, 2000.
[13] Li, Z.X.. Theory and Technique of Engineering Structural Testing. Tianjin: Tianjin Univ. Press, 2004.

STRENGTHENING OF COMPOSITE BEAM-TO-COLUMN JOINTS: STATIC AND SEISMIC BEHAVIOUR

G. LOHO
LGCGM - Structural Engineering Research Group, INSA
Rennes, France
Ghandi.Loho@yahoo.fr

A.LACHAL
LGCGM - Structural Engineering Research Group, INSA
Rennes, France
Alain.Lachal@insa-rennes.fr

J.M.ARIBERT
LGCGM - Structural Engineering Research Group, INSA
Rennes, France
jean-marie.aribert @insa-rennes.fr

ABSTRACT

This paper deals with the strengthening of beam-to-column end-plate bolted joints. Two strengthening dispositions have been developed and studied. The first one consists in adding a haunch welded on the beam bottom flange in the vicinity of the column. The second one consists in strengthening the column web panel (in presence or not of haunches) with double steel plates. This strengthening arrangement is studied in this paper from both experimental and numerical approaches. Based on these studies, two new static design models are proposed. The first model deals with the composite haunched joints. The second model provides a design method for the column panel zone strengthened by double steel plates.

INTRODUCTION

End-plate bolted beam-to-column joints are currently used in Europe in steel and composite construction. These joints often are semi-rigid and partial strength. The use of such joints in moment resisting frames in high ductility class (DCH) requires to strengthen them in order to make them rigid and full-strength. Besides EN 1998-3 [CEN, 2005] has specified recommendations, based on the works of [Yu et al. 2000], to strengthen beam-to-column steel connections of existing building by adding haunches.

Moment resisting frames subject to static or seismic lateral loads may develop large unbalanced moments in their beam-to-column joints and consequently high shear deformations in the column panel zone of these joints. In such a situation, the shearing of the panel zone has a significant influence on the moment-rotation behaviour of the joint and consequently should be taken into account in the global analysis of the structure (with regard to story drifts, second-order effects and stability) [Foutch DA 2002]. So, it is important to design properly the panel zone and therefore to control the resistance and the ductility of the joint. For that purpose doubler plates welded on the web column may be an appropriate solution. EN 1993-1-8 (clause 6.2.6.1) [CEN, 2005] gives some design rules to strengthen the column web panel by adding doubler plates. In order to calculate the shear resistance, this code defines a shear resistance area including parts of the column and the doubler plates cross-section. Nevertheless, EN 1993-1-8 limits the maximum thickness of the doubler plates to the thickness of the column web if the total thickness of the doubler plates exceeds the web thickness. In addition, EN 1993-1-8 assumes uniform distribution of shear stress within the panel zone.

Both approaches used to strengthen beam-to-column joints (doubler plates or/and haunches) are studied in this paper from an experimental program and a three-dimensional finite element modelling. On the basis of the numerical and experimental results, two new static design models are proposed here for each strengthening solution.

EXPERIMENTAL INVESTIGATION

Program of tests

An experimental program was carried out at INSA of Rennes-France to study the general behaviour of beam-to-column composite joints with emphasis on the effect of joint strengthening on its seismic performance. Two strengthening dispositions have been considered. The first one consists in extending the end-plate below the beam and adding adjacent haunches at the corners with the column. The second one consists in strengthening the column web panel (in presence or not of haunches) with double steel plates welded to the root radius of the column section with full penetration butt welds and welded to the column web by fillet welds (Figure 3).

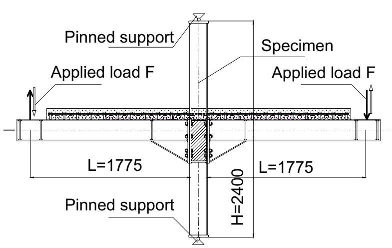

Fig. 1 – Haunched composite joint (Test G23)

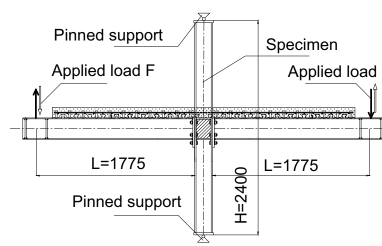

Fig. 2 – Extended end-plate composite joint (Tests G20 and G21)

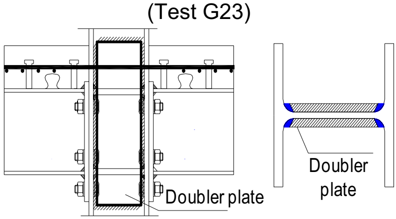

Fig. 3 – Arrangement of doubler plates strengthening the column web panel

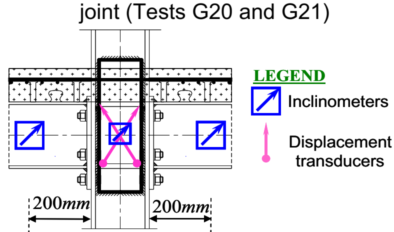

Fig. 4 – Locations of instrumentation

Figures 1 and 2 present the main characteristics of three full-scale beam-to-column joints G20, G21 and G23 (major axis connections) with cruciform arrangement. Common characteristics are a full shear connection for all composite specimens with welded headed studs Φ = 19 mm (h= 80 mm) and a composite slab (cast on a steel sheeting COFRASTRA 40) with a cross-section of dimensions 120×1000 mm. This slab is reinforced by 10 longitudinal rebars Φ10 mm and by transverse rebars Φ10 mm spaced each 10 cm. For all composite specimens, two doubler plates were connected to the column, as explained above, to strengthen the column web panel. Total doubler plate thicknesses are 2x6, 2x10 and 2x12mm in the three specimens G20, G21 and G23, respectively. All columns are HEB 200 steel sections and all steel beams are IPE 240. End-plate thickness is 15mm in the specimen G20 and 20mm in specimens G21 and G23. The joint rotations, column web panel distortion in shear and beam rotation are mainly deduced from inclinometers and linear displacement transducers (Figure 4). Bending moments in different cross-sections are determined from the measured actuator loads F multiplied by the appropriate lever arm L (Figures 1 and 2). In order to simulate the seismic action, the ECCS loading procedure [ECCS 1986] was followed. Two vertical loads were applied at each cantilever beam end on each side of the column by two hydraulic servo controlled actuators working out-of-phase in order to create loads acting in opposite direction.

Experimental results

For test G20 (without haunches) and test G23 (with haunches), the moment-rotation curves presented in Figures 5-a to f are only related to the right side of the joints. The bending moment $M_{j\,(Right)}$ is calculated at the load-introduction cross-section of the connection, i.e. the interface between end-plate and column flange. These moment-rotation curves show the respective contributions of the column panel zone ϕ_{Pa} (Figure 5-c and f) and the load-introduction cross-section (connection) $\phi_{li\,(Right)}$ (Figure 5-b and e) to the global joint rotation $\phi_{j\,(Right)}$ (Figure 5-a and d). Also, for test G23 (with haunches), the moment-rotation curve $M_b - \phi_b$ of the right beam (at the haunch tip) is illustrated in Figure 5-g. In Figure 5-h, we give the cyclic moment-rotation $M_{Pa} - \phi_{Pa}$ curve of the column panel zone in test G21 (without haunches). The moment M_{Pa} corresponds to the total moment acting in the joint ($M_{Pa} = M_{j\,(Right)} - M_{j\,(Left)}$). Also, Figure 5-h shows the skeleton curve and the curve obtained from EN 1993-1-8 [CEN, 2005] model. The results presented in Figures 5 to 8 allow to draw the following conclusions.

- Whereas the failure of full-strength joint G23 (with haunches) result from the rupture of the steel beam at the haunch tip (Figure 6) failures of partial-strength joints G20 and G21 (without haunches) occur by rupture in low-cycle fatigue of welds connecting beams to end-plates (Figure 7).
- For the specimen with full-strength joints (with haunches), joint rotations remain low in accordance with the small joint deformations observed during the tests (Figure 5-d); the main part of the rotation comes from the beam (Figure 5-g), providing a rotation capacity generally greater than 35 mrad (here, the rotation